Short Photoperiod-Induced Decrease of Histamine H3 Receptors Facilitates Activation of Hypothalamic Neurons in the Siberian Hamster

P. Barrett,* M. van den Top,* D. Wilson, J. G. Mercer, C. K. Song, T. J. Bartness, P. J. Morgan, and D. Spanswick

Rowett Institute of Nutrition and Health (P.B., D.W., J.G.M., P.J.M.), University of Aberdeen, Aberdeen AB21 9SB, United Kingdom; Division of Clinical Sciences (M.v.d.T., D.S.), Warwick Medical School, University of Warwick, Gibbet Hill Campus, Coventry CV4 7AL, United Kingdom; and Department of Biology (C.K.S., T.J.B.), Neurobiology and Behavior Program, Georgia State University, Atlanta, Georgia 30303-3083

Nonhibernating seasonal mammals have adapted to temporal changes in food availability through behavioral and physiological mechanisms to store food and energy during times of predictable plenty and conserve energy during predicted shortage. Little is known, however, of the hypothalamic neuronal events that lead to a change in behavior or physiology. Here we show for the first time that a shift from long summer-like to short winter-like photoperiod, which induces physiological adaptation to winter in the Siberian hamster, including a body weight decrease of up to 30%, increases neuronal activity in the dorsomedial region of the arcuate nucleus (dmpARC) assessed by electrophysiological patch-clamping recording. Increased neuronal activity in short days is dependent on a photoperiod-driven down-regulation of H3 receptor expression and can be mimicked in long-day dmpARC neurons by the application of the H3 receptor antagonist, clobenproprit. Short-day activation of dmpARC neurons results in increased c-Fos expression. Tract tracing with the trans-synaptic retrograde tracer, pseudorabies virus, delivered into adipose tissue reveals a multisynaptic neuronal sympathetic outflow from dmpARC to white adipose tissue. These data strongly suggest that increased activity of dmpARC neurons, as a consequence of down-regulation of the histamine H3 receptor, contributes to the physiological adaptation of body weight regulation in seasonal photoperiod. **(*Endocrinology* 150: 3655–3663, 2009)**

Food intake, growth, and reproduction are fundamental processes regulated through the hypothalamus (1). The neuroendocrine pathways involved are well described, but in addition, in seasonal mammals temporal inputs related to the ambient day length impose a further level of regulation on these axes so that major changes in food intake, body weight, growth, and reproduction are seen across an annual cycle in anticipation of climatic changes (2).

To accommodate a range of seasonal environmental conditions, seasonal mammals have evolved different strategies, from the extreme modification of physiology and behavior of hibernators to the more modest energy conserving mechanisms of nonhibernators, such as the Siberian hamster, involving inhibition of reproduction and reduced energy expenditure (3).

Whereas deep depression of central nervous system activity induced by elevated histamine and histamine H3 receptor expression underpins the extreme response of hibernators (4), the mechanisms involved in the interface between seasonal timing and the neuroendocrine pathways that regulate the major physiological axes in nonhibernating mammals are only beginning to be understood. Recent work has demonstrated that seasonal availability of hypothalamic thyroid hormone is a key event regulating seasonal adaptations (5–7), but little is known of the hypothalamic neuronal responses that lead to a change in behavior or physiology.

Recent studies of the Siberian hamster have revealed dynamic regulation of gene expression in response to prevailing seasonal photoperiod in a specific region of the arcuate nucleus of the

ISSN Print 0013-7227 ISSN Online 1945-7170
Printed in U.S.A.

doi: 10.1210/en.2008-1620 Received November 17, 2008. Accepted April 8, 2009.
First Published Online April 16, 2009
* P.B. and M.v.d.T. contributed equally to this work and are co-first authors.

Abbreviations: aCSF, Artificial cerebrospinal fluid; dmpARC, dorsomedial posterior arcuate nucleus; GABA, γ-aminobutyric acid; LD, long day; PRV, pseudorabies virus; SD, short day.

hypothalamus, the dorsomedial posterior arcuate nucleus (dmpARC) (8, 9). This region defined by the photoperiodic regulation of genes for H3 receptors and others (8, 9), lies close to the third ventricle between Bregma −2.7 through −2.3 mm based on the mouse brain atlas (10). Of the genes regulated by photoperiod in the dmpARC, the H3 receptor was found to be substantially decreased in short, winter-like photoperiod (9), suggesting a key role for histamine signaling through H3 receptors and a functional reorganization of the dmpARC with a directional change in photoperiod. Histamine H3 receptors are characteristically presynaptic in their action, acting as an autoreceptor for the release of histamine in tuberomamillary neurons and as a hetero-receptor for the release of a number of neurotransmitters including γ-aminobutyric acid (GABA) (11). Electrophysiological recording have characterized inhibition of high-threshold calcium currents and hyperpolarization due to activation of inwardly rectifying potassium currents as potential actions of H3 receptors in the inhibition of neurotransmitter release (12).

In this study, we combined electrophysiological recording techniques and analysis of the early response gene c-*fos*, a marker of cellular activation, to identify the central neural cellular signaling mechanisms in the dmpARC contributing to this behavioral shift to environmental change. Data presented here provide the first functional analysis of the dmpARC and reveal that this region of the ARC, which forms a component of the neural circuits regulating white adipose tissue via the sympathetic nervous system (13, 14), represents a novel and functionally distinct cell cluster, whose activity is regulated in a H3 receptor and photoperiod-dependent manner. These findings have important implications for the regulation of seasonal physiology, particularly adipose stores.

Materials and Methods

Animals

Male Siberian hamsters (*Phodopus sungorus*) of approximately 4 months of age were obtained from a breeding stock held at the Rowett Institute. All research using animals was licensed under the Animals (Scientific Procedures) Act of 1986 and received ethical approval from the Rowett Institute ethical review committee.

Male Siberian hamsters were individually housed at a constant temperature of 20 C with *ad libitum* access to food and water. Hamsters held in long day (LD) photoperiod were exposed to a light/dark cycle of 16-h light, 8-h darkness. Hamsters in short day (SD) photoperiod were exposed to a light/dark cycle of 8-h light, 16-h darkness. In a basic LD *vs.* SD comparison, hamsters were housed in their respective photoperiods for 14 wk by which time SD housed hamsters have achieved their nadir of body weight loss. At this time SD housed hamsters had reduced body weight by approximately 25%. Postmortem analysis was used to verify the expected SD-induced testicular regression before brains were subsequently used for *in situ* hybridization or electrophysiological recordings. In the switchback experiment, hamsters were housed in their respective photoperiods for 14 wk before transferring SD-exposed hamsters back to LD photoperiod. One group of hamsters were killed by cervical dislocation on the day of transfer and represent wk 0 of the switchback to LD. Groups of hamsters were then killed 2, 4, and 6 wk later.

For analysis of gene expression over a circadian cycle, hamsters held in LD or SD for 14 wk were killed at 3-h intervals over a 24-h period. This and previous studies have not found evidence of any effect of time of day on gene expression in the dmpARC. Therefore, hamsters were killed at midlight phase or ZT3 for *in situ* hybridization and electrophysiological studies.

In situ hybridization

In situ hybridization with a riboprobe for the detection of c-*fos* and the histamine H3 receptor was performed as described previously (15) with a ^{35}S-labeled antisense riboprobe. Slides were apposed to film for 7 d. Quantification of c-*fos* mRNA expression was by image analysis as described previously (5). Histological location of c-*fos* or H3 receptor expression was obtained by emulsion coating slides (LM1 emulsion; GE Healthcare, Amersham, UK) with development 21 d later.

Immunohistochemistry

Immunohistochemistry was performed on free floating sections cut at 30 μm as described previously (16). The primary antibody was a cross-reacting antihuman c-Fos antibody (Ab-5; Calbiochem, San Diego, CA) and was used at a 1:4000 dilution. Incubation with the primary antibody was for 48 h.

Pseudorabies virus (PRV) tracing from white adipose tissue

These experiments have been described in detail elsewhere (14). All procedures were approved by the Georgia State University Institutional Animal Care and Use Committee and are in accordance with Public Health Service and U.S. Department of Agriculture guidelines. Briefly, hamsters were exposed to a LD photoperiod (16 h light, 8 h dark cycle; lights on at 0200 h) from birth and kept at 21 ± 2 C. PMI Rodent Diet no. 5001 (Purina, St. Louis, MO) and tap water were provided *ad libitum* throughout the study. Hamsters were single housed 1 wk before inguinal white adipose tissue PRV injections.

Hamsters were anesthetized with pentobarbital sodium (50 mg/kg) and the target incision area over the rear haunch area was shaved and wiped with 70% ethanol. An incision was made at the dorsal hind limb of the animal and lateral to the spinal column that continued rostrally and then ventrally to the ventral hind limb. Care was taken with the depth of the incision so as to not damage the underlying fat pad and vasculature.

PRV injections

Once the inguinal white adipose tissue pad was exposed, a series of injections of PRV 152 (generous gift of Lynn Elmquist, Princeton, NJ) was made using a 1.0-μl microsyringe at five loci within the fat pad (1.5×10^8 pfu/ml; 150 nl/loci) to evenly distribute the virus. The incision was closed with sterile wound clips and nitrofurazone powder was applied to minimize the risk of sepsis. The animals were then transferred to clean cages for 6 d, the postinoculation survival time for infection to reach the rostral forebrain from these fat pads in this species.

Six days after PRV injections, animals were given an overdose of pentobarbital sodium (300 mg/kg ip) and perfused transcardially with heparinized (0.02%) saline and phosphate buffered (0.1 M; pH 7.4) paraformaldehyde (4% wt/vol). The brains were extracted and postfixed in the same fixative overnight at 4 C and sunk in sucrose (30% wt/vol; with 0.1% sodium azide). The brains were sliced at 30 μm using a freezing stage sliding microtome along the coronal plane and kept in cryoprotectant until processed for immunohistochemistry to detect PRV labeling.

Immunohistochemistry for single-label PRV

Brain sections were rinsed multiple times in PBS (0.1 M; pH 7.4) and then incubated in the primary antibody (rabbit anti-PRV; Rb132; 1:10,000; a generous gift of Lynn Enquist, Princeton, NJ) overnight. The secondary antibody (goat antirabbit; 1:500; Vector Laboratories, Burlingame, CA) was applied for 2 h, and then the sections were placed in avidin-biotin complex (Vector) for 1 h. The specific labels were detected using diaminobenzidine (0.1 mg/ml; Sigma, St. Louis, MO) as the chromogen in the presence of hydrogen peroxide (0.0025%). All steps in the immunohistochemistry procedure were performed at 22 C. The sections

were mounted onto gelatin-coated slides and air dried. Staining for PRV was observed from the level of the preoptic area rostrally and through the brain stem caudally using a BX41 microscope (Olympus, Tokyo, Japan). Images were captured digitally with an Olympus DP70 camera and acquired using Adobe Photoshop (version 6.0; San Jose, CA). A mouse brain atlas was used as a guide to identify brain regions (17). To determine the percentage of cells infected by PRV, PRV-immunostained cells were counted in every sixth section of 25 μM sections taken through the arcuate nucleus in three different LD hamsters. The sub-divisions of the arcuate nucleus were based on those of Franklin and Paxinos (10) with the exception of the region termed the dmpARC.

Electrophysiology

Slice preparation

Whole-cell electrophysiological recordings from neurons in the arcuate nucleus in isolated brain slices were obtained using methods similar to those described in detail previously (18–20). The brain was rapidly removed from hamsters maintained under LD or SD conditions for 14 wk. Coronal 350-μm slices containing the dmpARC were cut from the isolated brain using a Vibratome (series 1000; Intracel, Royston, UK). Slices were maintained at room temperature in oxygenated artificial cerebrospinal fluid (aCSF) for at least an hour before recording.

Recording and analysis

For recording, slices were transferred to a custom-made recording chamber and continuously perfused at room temperature with aCSF of the following composition (in millimoles): 127.0 NaCl, 1.9 KCl, 1.2 KH_2PO_4, 26.0 $NaHCO_3$, 10.0 D-glucose, 1.3 $MgCl_2$, 2.4 $CaCl_2$, equilibrated with 95% O_2, 5% CO_2 (pH 7.3–7.4). Recordings were obtained from neurons located in the dmpARC using axopatch-1D amplifiers (Axon Instruments, Foster City, CA). Patch pipettes were pulled using a horizontal puller (Sutter Instrument Co., Novato, CA) from thin-walled borosilicate glass (Harvard apparatus, Ltd., Edenbridge, Kent, UK) with resistances between 4 and 7 MΩ when filled with electrode solution. The pipette solution comprised (in millimoles); 140.0 potassium gluconate, 10.0 HEPES, 10.0 KCl, 1.0 EGTA, 4.0 Na-ATP (pH 7.4). Current and voltage data were displayed on a digital oscilloscope (Gould DSO1602) and stored on DAT-tape (Biological DTR-1204; Intracel) and as a digital file on the computer. For data analysis, signals were digitized at 2–10 kHz, stored, and analyzed on a personal computer running pClamp8 software (Axon Instruments).

Drugs and solutions

Drugs used were imetit and clobenpropit (Tocris Bioscience, Bristol, UK). These were chosen on the basis of their affinity and ability to inhibit (imetit) cAMP activation by the cloned Siberian hamster H3 receptors (long and short splice variants) or for clobenpropit, antagonism of R-methylhistamine inhibition of cAMP stimulation by forskolin (Ref. 9 and Barrett, P., unpublished data). Although both ligands have been reported to have agonist activity at the histamine H4 receptor, activity at this receptor is ruled out in these studies as H4 receptors are not expressed in the brain (21, 22). Stock solutions of the drugs were made in distilled water before dilution in aCSF. All drugs were bath applied from reservoirs connected to the aCSF flow line by manually operable three-way valves.

Statistical analyses

All values are expressed as mean ± SEM. The two-tailed Student's *t* test was used for all statistical analysis in the paired and independent configuration as appropriate. All statistics were performed on a personal computer running Microsoft Excel (Richmond, CA).

Results

Photoperiodic regulation of c-Fos and innervation of white adipose tissue by hypothalamic dmpARC neurons

In situ hybridization studies using an antisense *c-fos* riboprobe on brain sections from Siberian hamsters held in LD photoperiod (16 h light, 8 h dark) or SD photoperiod (8 h light, 16 h dark) for 14 wk revealed expression of the immediate early gene c-*fos* in the dmpARC of SD hamsters, with no detectable expression in LD hamsters (Fig. 1, A and B). This suggests selective activation of neurons in the dmpARC of SD hamsters. Immunohistochemical localization of c-Fos protein confirmed expression exclusively in SD hamsters consistent with c-*fos* mRNA up-regulation (Fig. 1C). To eliminate the possibility of changes in c-*fos* expression reflecting differences in circadian expression between the two lighting schedules, *in situ* hybridization was performed on brain sections from hamsters culled at 3-h intervals over a 24-h period. No c-*fos* expression was observed at any time during the circadian cycle in LD, whereas expression was observed at all time points in SD with no strong circadian variation, suggesting constitutive expression in the dmpARC (Fig. 1D). Analysis of c-*fos* expression in hamsters switched from SD to LD following 14 wk of SD photoperiod exposure revealed a rapid decline to almost undetectable levels of c-*fos* expression by 6 wk of LD exposure, with an inverse relationship to the photoperiod-driven testicular and body weight change (Fig. 1E).

Song and Bartness (14) previously demonstrated sympathetic innervation of white adipose tissue using the retrograde tract tracing ability of PRV injected into adipose tissue of the hamster. Analysis of brain sections from these experiments revealed that dmpARC neurons are infected by PRV, demonstrating sympathetic innervation of white adipose tissue by neurons originating in the dmpARC (Fig. 2, A and B). Counting of PRV infected neurons in sub-divisions of arcuate nucleus (Fig. 2) identify approximately 14% of all PRV infected neurons to be located in the dmpARC (Table 1).

Photoperiod regulates the activity of neurons in the dmpARC

Whole-cell patch clamp recording techniques on *in vitro* hypothalamic brain slice preparations revealed that spontaneous action potential firing was significantly higher in SD than LD dmpARC neurons (Fig. 3A), average firing frequency amounting to 3.6 ± 0.5 Hz in SD compared with 0.7 ± 0.1 Hz in LD neurons (n = 50, $P < 0.001$, independent two tailed student *t* test; Fig. 3D). Increased neuronal activity in SD dmpARC neurons was associated with a significant increase in membrane resistance, amounting to 2730 ± 159 MΩ in SD compared with 1764 ± 79 MΩ in LD (n = 50, $P < 0.001$, Fig. 3, B–D). Increased activity in SD dmpARC neurons was therefore consistent with observations of increased c-*fos* expression in these animals and consistent with a mechanism involving inhibition or down-regulation of one or more conductances, resulting in increased spontaneous activity in SD dmpARC neurons. This observation together with our previous report of photoperiod-dependent down-regulation of mRNA for his-

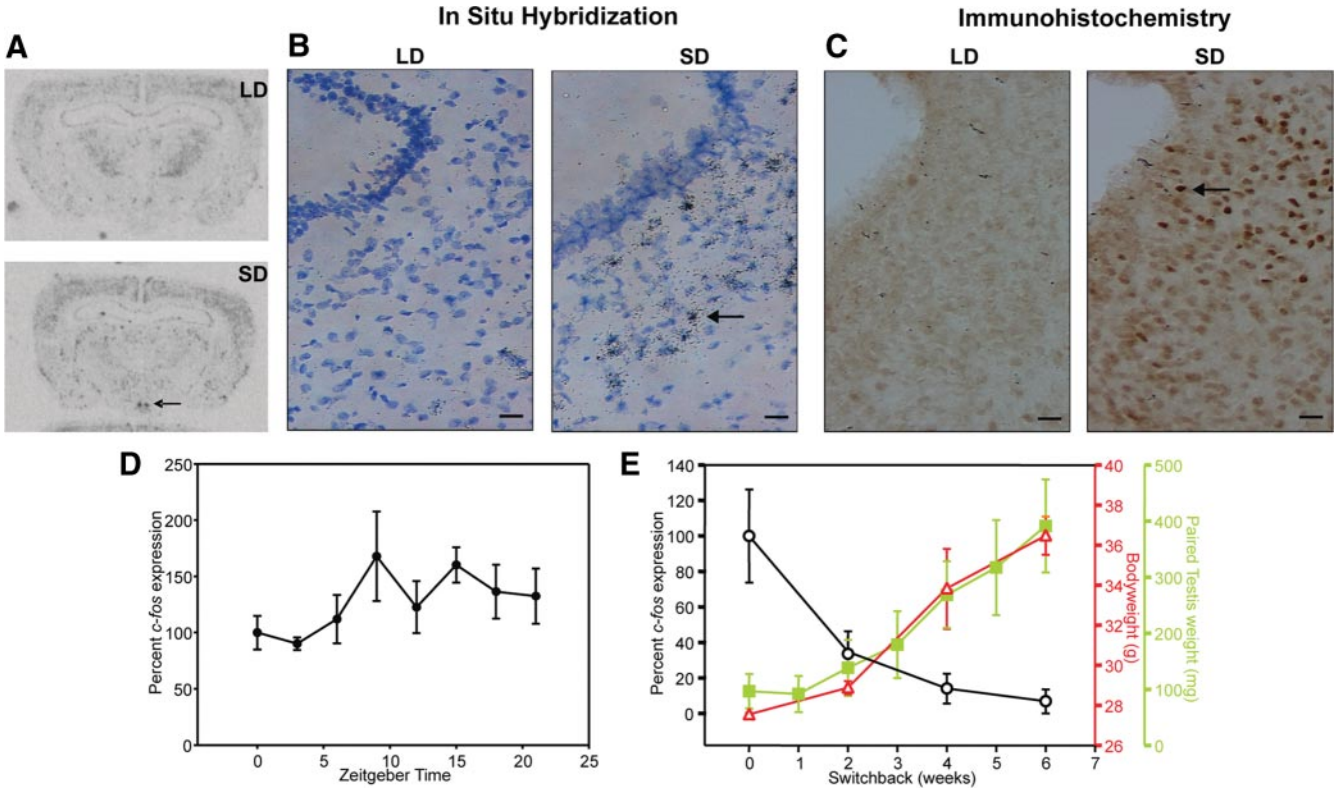

FIG. 1. Neuronal activation, indicated by c-*fos* expression, in the dmpARC correlates with a LD to SD shift in photoperiod. A, Autoradiography of c-*fos* antisense riboprobe *in situ* hybridization to Siberian hamster brain sections housed in LD and SD photoperiod, respectively. *Arrow* indicates dmpARC. B, Emulsion-coated sections of LD and SD brain sections, respectively, enlarged to show the hybridization signal in the region of the dmpARC (*arrow*). C, Immunohistochemistry on perfused LD and SD. Siberian hamster brain sections with a c-*Fos* antibody (*dark brown*) in the region of the dmpARC. *Arrow* indicates example of immunostained c-*Fos* positive neuron. D, Analysis of c-*fos* expression over the course of a 24-h light-dark cycle. Shown are the values of c-*fos* expression in a SD light-dark cycle. No difference in the expression was observed in a 24-h LD light-dark cycle. E, Graph plotting the inverse relationship of c-*fos* expression to photoperiod changes in testis weight and body weight. *Scale bars* (B and C), 20 μM.

tamine H3 receptors after a switch from LD and SD photoperiod (9) led to the hypothesis that changes in the functional expression of H3 receptors contribute to changes in activity of dmpARC neurons.

H3 receptors modulate photoperiod-regulated activity of dmpARC neurons

The H3 receptor agonist, imetit (200 nM), applied to hypothalamic slices inhibited spontaneous action potential discharge

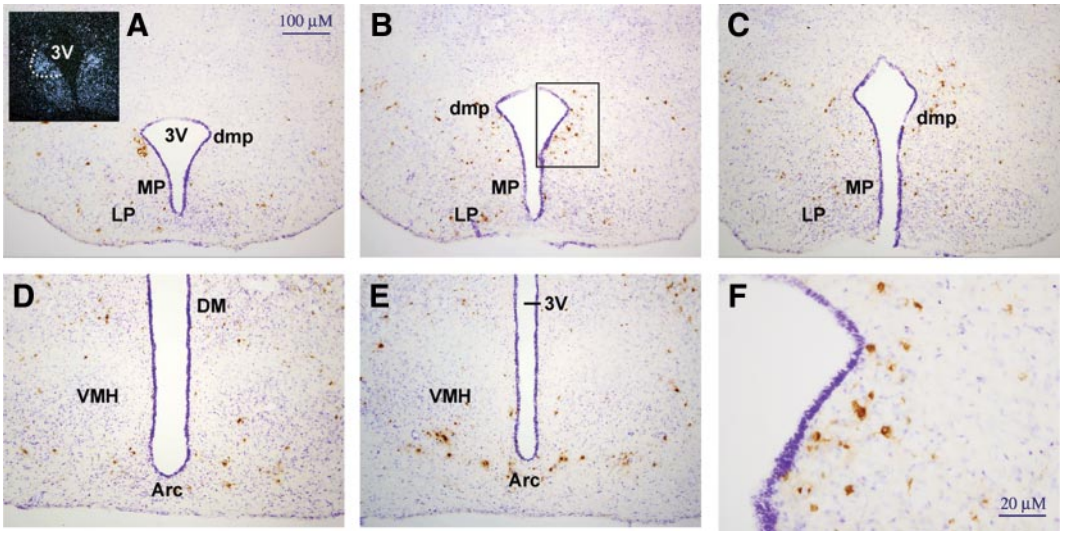

FIG. 2. Retrograde labeling of arcuate nucleus neurons after injection of PRV into adipose tissue fat pads. A–E, Immunostained PRV-infected neurons through the arcuate nucleus. Subdivisions are indicated. *Insert* (A) is a dark-field image of an *in situ* hybridization performed for histamine H3 receptor to illustrate the location of the dmpARC and the relative locations of the labeled histamine H3 receptor-labeled neurons with PRV-infected neurons. The location defined as the dmpARC is outlined by a *dotted line*. F, A higher magnification image of the area boxed in image (B) showing PRV infected neurons in the dmpARC. 3V, Third ventricle; LP, lateral posterior arcuate nucleus; MP, medial posterior arcuate nucleus; dmp, dorsomedial posterior arcuate nucleus; DM, dorsomedial nucleus; VMH, ventral medial nucleus; Arc, arcuate nucleus.

TABLE 1. Percentage of PRV-infected neurons in subdivisions of the arcuate nucleus

Arcuate nucleus subdivision	Average (%) ± SEM
Arc	28.10 ± 12.83
Arc D	4.47 ± 1.02
Arc L	10.49 ± 1.08
Arc MP	24.00 ± 4.79
Arc LP	18.59 ± 5.54
Arc dmp	14.35 ± 2.17
Total	100

The percentage was determined by counting immunostained PRV-infected neurons in each region of the arcuate nucleus (Arc) in every sixth section of 25 μM sections through the arcuate nucleus in three LD Siberian hamsters. The subdivisions are defined according the mouse brain atlas (10) with the exception of the dmpARC. Arc D, Dorsal arcuate nucleus; Arc L, lateral arcuate nucleus; Arc MP, Medical posterior arcuate nucleus; Arc LP, lateral posterior arcuate nucleus.

in LD dmpARC neurons, from 0.54 ± 0.14 Hz in control to 0.01 ± 0.01 Hz in the presence of imetit (n = 11 of 18). The response was characterized by a 5.1 ± 1.2 mV membrane potential hyperpolarization, from −42.8 ± 1.6 to −47.9 ± 1.8 mV in the presence of imetit (n = 11, Fig. 4A), associated with a 28% reduction in membrane resistance from 1639 ± 270 to 1188 ± 183 MΩ (Fig. 4, A and C). The H3 receptor antagonist, clobenpropit (10 μM), induced an increase in suprathreshold neuronal activity from 0.23 ± 0.13 to 0.65 ± 0.21 Hz and a 4.4 ± 0.7 mV membrane depolarization from a resting membrane potential of −45.3 ± 1.8 to −40.9 ± 1.6 mV (n = 9 of 14, Fig. 4, B and C). Clobenpropit-induced depolarization was associated with a 21% increase in membrane resistance from a control value of 1185 ± 105 to 1432 ± 183 MΩ (n = 7). In contrast to the effects of H3 receptor ligands in LD dmpARC neurons, neither imetit (22 of 23) or clobenpropit (13 of 15) induced significant effects in SD dmpARC neurons (Fig. 4, A, and B). The firing frequency of SD dmpARC neurones before application of imetit was 3.0 ± 0.7 and 2.8 ± 0.7 Hz in the presence of imetit (n = 23). The membrane potential and input resistance of these neurones was −44.5 ± 0.6 mV (n = 23) and 2021 ± 201 MΩ, respectively (data from Ref. 11), in the absence of imetit and −44.7 ± 0.6 mV and 1927 ± 190 MΩ, respectively, in the presence of the agonist.

Bath application of clobenpropit had no significant effect on firing frequency in SD hamsters, firing frequency amounting to 3.4 ± 0.6 Hz in control and 3.3 ± 0.5 Hz in the presence of clobenpropit (n = 15). Similarly, clobenpropit was without effect on membrane potential (control −44.2 ± 1.0 mV; clobenpropit −44.0 ± 1.0 mV, n = 15) and input resistance (control 1603 ± 107 MΩ; clobenpropit 1609 ± 83 MΩ, data from Ref. 11) in SD hamsters. These data suggest that H3 receptors contribute to the maintenance of low levels of activity in LD dmpARC neurons and that their subsequent down-regulation in SD neurons contributes to the increased level of activity associated with this photoperiod.

Current-voltage relations before and in the presence of imetit revealed a conductance increase in the presence of the agonist associated with a reversal potential of −63.1 ± 1.6 mV (n = 9, Fig. 5A). Current-voltage relations in the absence and presence of clobenpropit revealed a decrease in conductance, consistent with ion channel closure, and a reversal potential of −62.2 ± 9.1 mV (n = 5, Fig. 5B). Thus, the reversal potential for both imetit- and clobenpropit-induced membrane responses were close to but negative from the reversal potential of chloride ions under our recording conditions.

The involvement of $GABA_A$ and $GABA_B$ receptors in the H3-mediated inhibition of the dmpARC was investigated in three clobenpropit-excited LD dmpARC neurones. In these neurones, clobenpropit induced a readily reversible 6.1 ± 0.6 mV membrane depolarization from a resting membrane potential of

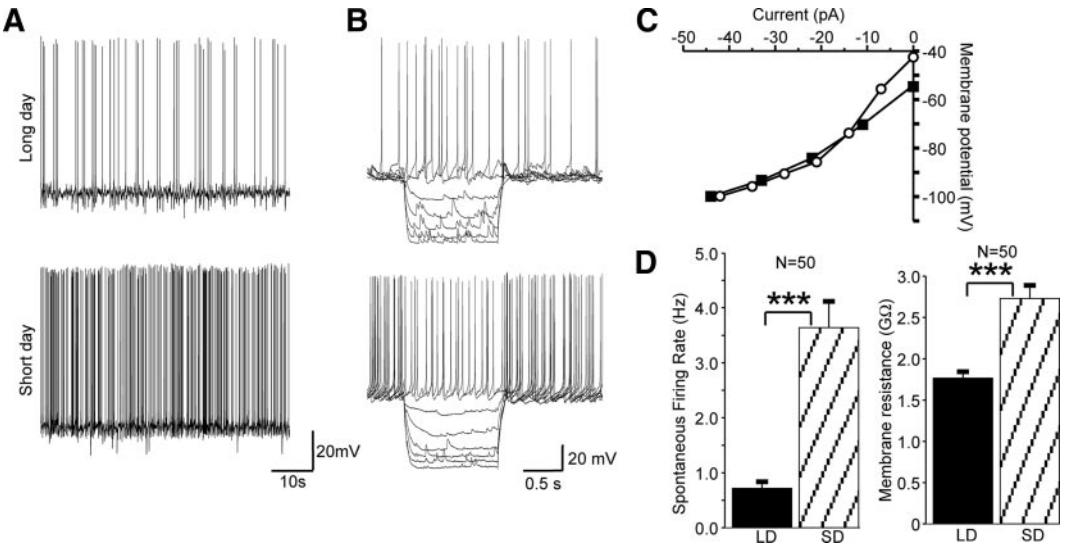

FIG. 3. Increased neuronal activity in dmpARC neurons correlates with a LD to SD shift in photoperiod. A, Continuous records from two neurons illustrating spontaneous action potential firing is significantly lower in LD *vs.* SD photoperiods. B, Superimposed electrotonic potentials evoked in response to current pulse injection of variable amplitude (not shown) in LD (*top*) and SD (*bottom*) photoperiod revealed increased activity in SD neurons was associated with an increase in input resistance, suggesting closure of ion channels in SD *vs.* LD. C, Corresponding voltage-current relations. Note the increased slope in the SD dmpARC neuron, indicating a higher input resistance (*open circles*) than the corresponding neuron in LD (*closed squares*). D, Summary overview of the averaged data for firing rate and membrane resistance showing the significant increase in these membrane properties in SD *vs.* LD photoperiods. ***, Significance at $P < 0.001$).

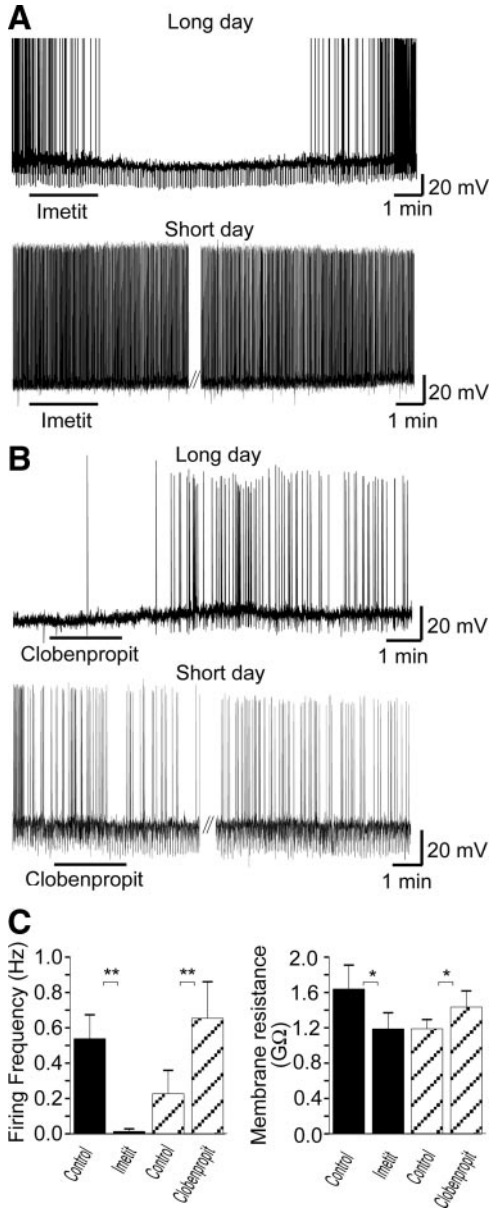

FIG. 4. H3 receptor-mediated signaling regulates neuronal activity of dmpARC neurons in LD but not SD photoperiods. A, Continuous records from two dmpARC neurons showing the H3 receptor agonist imetit-induced inhibition in a LD dmpARC neuron (*top*) but was without effect on a SD dmpARC neuron (*bottom*). B, Continuous record showing the H3 receptor antagonist/partial agonist clobenpropit-induced excitation of a LD dmpARC neuron (*top*) and was without effect in SD dmpARC neurons (*bottom*). The downward deflections in membrane potential in A (*top*) and B (*bottom*) are the result of repetitive rectangular-wave constant current injections (0.2Hz, −10 pA, 0.5 sec) used to monitor changes in membrane resistance. C, Bar charts summarizing the effects of imetit (*filled bars*) and clobenpropit (*diagonal bars*) on firing rate (*left*) and membrane resistance (*right*) in LD hamsters. Imetit significantly decreased firing rate and input resistance, whereas clobenpropit increased firing rate and input resistance, suggesting mechanisms mediated through opening and closing of ion channels, respectively. *, $P < 0.05$; **, $P < 0.005$.

−53.4 ± 4.9 mV (n = 3). After this response, the membrane potential recovered to −54.0 ± 4.4 mV (n = 3, Fig. 5C). The membrane depolarization was associated with a 25% increase in membrane resistance from a control value of 1157 ± 225 to 1455 ± 303 MΩ (n = 3, Fig. 5C). Application of the combination of bicuculline (antagonist for $GABA_A$ receptor) and 2-OH-saclofen (antagonist for the $GABA_B$ receptor) mimicked the clobenpropit-induced membrane depolarization previously observed in the same neurons (Fig. 5C). In the presence of bicuculline and 2-OH-saclofen the membrane was depolarized by 10.3 ± 3.6 mV from a resting membrane potential of −53.8 ± 5.0 mV (n = 3). The depolarization was associated with a 34 ± 13% increase in membrane resistance from a control value of 917 ± 133 to 1240 ± 251 MΩ (n = 3). Subsequent application of clobenpropit in the presence of bicuculline and 2-OH-saclofen failed to induce a membrane response (Fig. 5C, n = 3; membrane potential: control, −55.9 ± 5.5 mV, clobenpropit, −55.3 ± 4.4 mV and membrane resistance: control, 965 ± 172 MΩ, clobenpropit, 963 ± 120 MΩ). These results show that tonic activation of histamine H3 and GABA receptors under LD conditions underlies the reduced excitability of dmpARC neurons.

Discussion

The arcuate nucleus of the hypothalamus has been the target of extensive research reflecting its importance in the central control of energy balance and reproduction and as a center in which these vital processes are integrated (23–26). Our data show that a functionally distinct subpopulation of neurons in the dmpARC is differentially active during different photoperiods and that this activity is dependent on photoperiod-regulated expression of histamine H3 receptors.

The early response gene, c-*fos*, extensively used as a marker of neuronal activation was constitutively expressed in SD dmpARC neurons. Expression of c-*fos* is inversely related to H3 receptor expression in the dmpARC (9). These data together with electrophysiological and pharmacological data described in the current paper indicate a pivotal role for this receptor and changes in activity in a functional reorganization these neurons.

It was important to ascertain the expression of c-*fos* over the course of 24 h because previous studies indicated c-*fos* is expressed with a circadian rhythm in proopiomelanocortin arcuate neurons (27, 28) and also to rule a time-dependent effect relative to seasonal photoperiod. The expression of c-*fos* was sustained over the course of a 24-h period without any significant circadian variation, indicating these neurons are likely to be continually activated in SD hamsters. No expression was observed at any time point in LD hamsters. This demonstrates that activity in dmpARC neurons is photoperiod dependent. Our previous studies have shown changes in gene expression in the dmpARC are dependent on the presence of the pineal gland and melatonin (8, 9), the principal hormone synthesized by the pineal gland during the hours of darkness. *In situ* hybridization studies have not revealed melatonin receptors to be expressed on dmpARC neurons, and therefore, these neurons are likely to be regulated by a more generic mechanism. One candidate for such a mechanism is the photoperiod regulated availability of thyroid hormone (5).

Whole-cell patch clamp recording from dmpARC neurons showed the spontaneous firing rate of these neurons to be

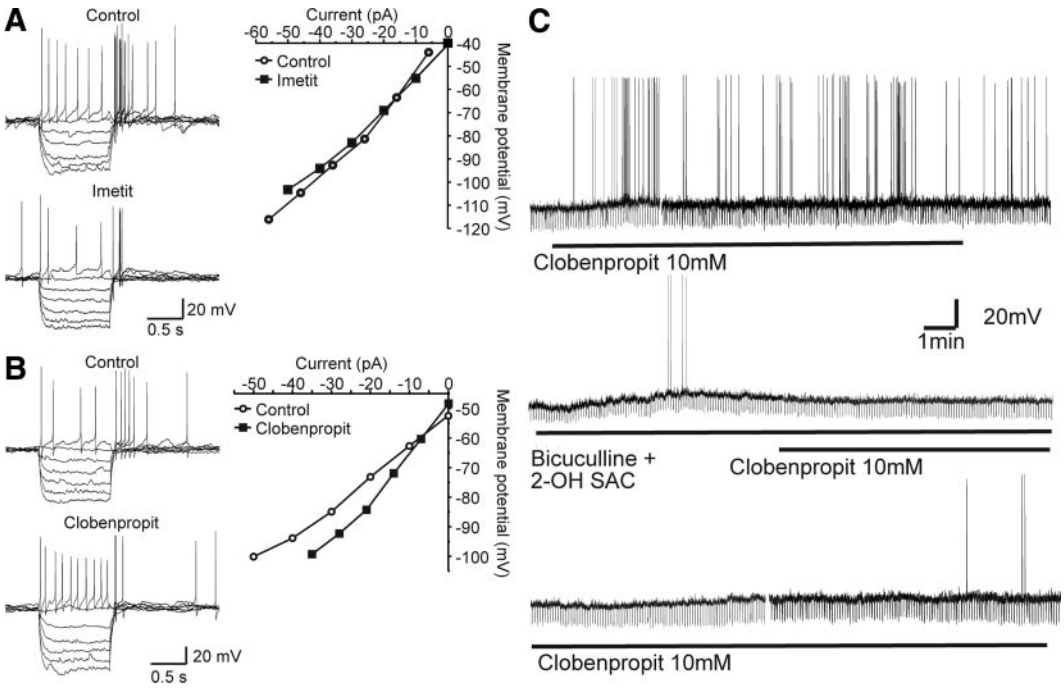

FIG. 5. H3 receptors in LD dmpARC neurons modulate neuronal activity via a chloride-dependent mechanism. A, Samples of a continuous record showing superimposed electrotonic potentials evoked in response to current injection in the absence (*top*) and presence of imetit (*bottom*). *Right*, Corresponding voltage-current relations (control, *closed squares*; imetit, *open circles*). B, Samples of a continuous record showing superimposed electrotonic potentials evoked in response to current injection in the absence (*top*) and presence of clobenpropit (*bottom*). *Right*, Corresponding voltage-current relations (control, *closed squares*; clobenpropit, *open circles*). Note plots in both A and B intersect around −60 mV, close to the reversal potential for chloride ions under our recording conditions. C, *Top trace*, depolarization of dmpARC neurones by clobenpropit; *middle trace*, the application of a combination of bicuculline and 2-OH-saclofen mimicked the clobenpropit-induced membrane depolarization previously observed in the same neurons (*top trace*). Subsequent application of clobenpropit in the presence of bicuculline and 2-OH-saclofen failed to induce a membrane response. *Bottom trace* Upon washout of bicuculline and 2-OH-saclofen, the clobenpropit responsiveness was restored. Shown is a representative trace (one of three) of responses to drug applications performed in a dmpARC neuron.

increased by 500% in SD. H3 receptor agonists and antagonists were effective in LD dmpARC neurons, the latter inducing increases in firing rate indicating that a tonic inhibitory drive mediated through these receptors contributes to suppression of spontaneous activity in the dmpARC in the long, summer-like, photoperiod. Conversely, H3 receptor ligands were without effect in SD neurons, consistent with the decreased expression of histamine H3 receptors in the short, winter-like, photoperiod in the dmpARC (9) and increased electrical activity as a result of the reduced tonic inhibitory drive mediated through these receptors.

The application of $GABA_A$ and $GABA_B$ receptor antagonists in LD slices mimicked the response obtained with clobenpropit, inducing a similar membrane depolarization and increase in membrane resistance. These data indicate that H3 receptors when expressed in LD, use a mechanism ultimately involving tonic GABA release and activation of postsynaptic GABA receptors to suppress the activity of dmpARC neurons. Further work is required to fully identify the mechanisms and site of action by which histamine, through H3 receptors, modifies GABA-mediated synaptic transmission at the level of the dmpARC.

Tract tracing using the retrograde tracer PRV demonstrates neurons located in the dmpARC ultimately project to white adipose tissue. Photoperiod-induced adaptations to seasonal variation in food availability and temperature, involves a reduction in food intake and mobilization of fat stores (3). The innervation of white adipose tissue by sympathetic nerves in turn innervated by fibers arising from the dmpARC that are constitutively active is consistent with a role for these neurons in the seasonal mobilization of fat stores. Furthermore, the activity of dmpARC neurons is inversely related to body weight when lean SD hamsters are switched from SD to LD and increase body weight. The percentage infection of dmpARC neurons compares favorably to larger subdivisions of the arcuate nucleus (10), in which, for example, 28% of neurons are infected by PRV in the medial posterior subdivision, in which neuropeptide Y neurons are principally located and 18% are infected by PRV in the lateral posterior subdivision.

The arcuate nucleus and in particular dmpARC neurons, however, form one component of the neural circuits innervating and regulating the sympathetic nervous input to white adipose tissue, identified by PRV track tracing (14). Therefore, dmpARC neurons likely do not function in isolation but are part of a larger network of premotor sympathetic neurons arising from other hypothalamic nuclei including the paraventricular nucleus, dorsomedial nucleus, and zona incerta, which express melatonin receptors and which could be influenced directly by the change in duration of the melatonin signal (11). Nevertheless, our findings are consistent with a role for histamine and H3 receptors in the regulation of seasonal behavior and physiology as found in hibernating mammals (4, 29). Furthermore, these data are also consistent with a role for histamine and H3 receptors in food intake and body weight. This proposition is supported by several

lines of evidence including the presence of histaminergic projections from the tuberomamillary nucleus to hypothalamic centers involved in regulating satiety, food intake, and energy homeostasis (30), including the arcuate nucleus (31); H3 receptor expression in hypothalamic areas involved in the control of energy homeostasis including the dmpARC (7, 32); reduced food intake after pharmacological inhibition of H3 receptors with antagonists (33–36); and proposals that H3 receptor ligands may have utility as antiobesity and antidiabetic therapies (37, 38). Thus, we provide data indicating a novel mechanism of action of histamine acting via H3 receptors in a specific subpopulation of arcuate nucleus neurons that are very responsive to change in photoperiod as evidenced by a large number of genes showing dynamic regulation to photoperiod in a single area of the hamster brain.

At present we do not know whether down-regulation of H3 receptor is independent of, or is solely responsible for, the emergence of c-*fos* expression or may involve activation of a cAMP pathway via Gs- and Gq-coupled receptors melanocortin 3 receptor, 5-hydroxytryptamine-7, and 5-hydroxytryptamine-2A, which we have recently shown to increase in expression in the dmpARC in SD hamsters (39). Nevertheless, taken together, these observations suggest that this specific area of the brain is important to the coordination of major adaptations in physiology and behavior associated with the annual cycle of environmental change in the Siberian hamster.

Acknowledgments

We thank Dr. Dawn Collins for comments and assistance with the preparation of the manuscript.

Address all correspondence and requests for reprints to: Dr. Perry Barrett, University of Aberdeen, Rowett Institute of Nutrition and Health, Greenburn Road, Bucksburn, Aberdeen AB21 9SB, United Kingdom. E-mail: p.barrett@abdn.ac.uk; or d.spanswick@warwick.ac.uk.

This work was supported by the Scottish Government Rural and Environment Research and Analysis, the European Union as part of Framework VII: LSHM-CT-2003-503041, "Diabesity Integrated Project" (Aberdeen), Biotechnology and Biological Sciences Research Council (Warwick), and the National Health Service (Warwick).

Disclosure Summary: The authors have nothing to disclose.

References

1. **Schneider JE** 2004 Energy balance and reproduction. Physiol Behav 81:289–317
2. **Prendergast BJ, Nelson RJ, Zucker I** 2002 Mammalian seasonal rhythms: behavior and neuroendocrine substrates. In: Pfaff D, Arnold A, Etgen A, Fahrbach S, Rubin R, eds. Hormones, brain and behaviour. Vol. II. San Diego: Academic Press; 93–156
3. **Morgan PJ, Ross AW, Mercer JG, Barrett P** 2006 What can we learn from seasonal animals about the regulation of energy balance? Prog Brain Res 153: 325–337
4. **Sallmen T, Beckman AL, Stanton TL, Eriksson KS, Tarhanen J, Tuomisto L, Panula P** 1999 Major changes in the brain histamine system of the ground squirrel, *Citellus lateralis*, during hibernation. J Neurosci 19:1824–1835
5. **Barrett P, Ebling FJ, Schuhler S, Wilson D, Ross AW, Warner A, Jethwa P, Boelen A, Visser TJ, Ozanne DM, Archer ZA, Mercer JG, Morgan PJ** 2007 Hypothalamic thyroid hormone catabolism acts as a gatekeeper for the seasonal control of body weight and reproduction. Endocrinology 148:3608–3617
6. **Yoshimura T, Yasuo S, Watanabe M, Iigo M, Yamamura T, Hirunagi K, Ebihara S** 2003 Light-induced hormone conversion of T_4 to T_3 regulates photoperiodic response of gonads in birds. Nature 426:178–181
7. **Viguié C, Battaglia DF, Krasa HB, Thrun LA, Karsch FJ** 1999 Thyroid hormones act primarily within the brain to promote the seasonal inhibition of luteinizing hormone secretion in the ewe. Endocrinology 140:1111–1117
8. **Ross AW, Webster CA, Mercer JG, Moar KM, Ebling FJ, Schuhler S, Barrett P, Morgan PJ** 2004 Photoperiodic regulation of hypothalamic retinoid signaling: association of retinoid X receptor γ with body weight. Endocrinology 145:13–20
9. **Barrett P, Ross AW, Balik A, Littlewood PA, Mercer JG, Moar KM, Sallmen T, Kaslin J, Panula P, Schuhler S, Ebling FJ, Ubeaud C, Morgan PJ** 2005 Photoperiodic regulation of histamine H3 receptor and VGF messenger ribonucleic acid in the arcuate nucleus of the Siberian hamster. Endocrinology 146:1930–1939
10. **Franklin K, Paxinos G** 1997 The mouse brain in sterotactic coordinates. San Diego: Academic Press
11. **Garcia M, Floran B, Arias-Montaño JA, Young JM, Aceves J** 1997 Histamine H3 receptor activation selectively inhibits dopamine D1 receptor-dependent [3H]GABA release from depolarization-stimulated slices of rat substantia nigra pars reticulata. Neuroscience 80:241–249
12. **Brown RE, Stevens DR, Haas HL** 2001 The physiology of brain histamine. Prog Neurobiol 63:637–672
13. **Bamshad M, Aoki VT, Adkison MG, Warren WS, Bartness TJ** 1998 Central nervous system origins of the sympathetic nervous system outflow to white adipose tissue. Am J Physiol 275:R291–R299
14. **Song CK, Bartness TJ** 2001 CNS sympathetic outflow neurons to white fat that express MEL receptors may mediate seasonal adiposity. Am J Physiol Regul Integr Comp Physiol 281:R666–R672
15. **Morgan PJ, Webster CA, Mercer JG, Ross AW, Hazlerigg DG, MacLean A, Barrett P** 1996 The ovine pars tuberalis secretes a factor(s) that regulates gene expression in both lactotropic and nonlactotropic pituitary cells. Endocrinology 137:4018–4126
16. **Tups A, Helwig M, Stöhr S, Barrett P, Mercer JG, Klingenspor M** 2006 Photoperiodic regulation of insulin receptor mRNA and intracellular insulin signaling in the arcuate nucleus of the Siberian hamster, *Phodopus sungorus*. Am J Physiol Regul Integr Comp Physiol 291:R643–R650
17. **Franklin K, Paxinos G** 1997 The mouse brain in sterotactic coordinates. San Diego: Academic Press
18. **Spanswick D, Smith MA, Mirshamsi S, Routh VH, Ashford ML** 2000 Insulin activates ATP-sensitive K+ channels in hypothalamic neurons of lean, but not obese rats. Nat Neurosci 3:757–758
19. **Spanswick D, Smith MA, Groppi VE, Logan SD, Ashford ML** 1997 Leptin inhibits hypothalamic neurons by activation of ATP-sensitive potassium channels. Nature 390:521–525
20. **van den Top M, Lee K, Whyment AD, Blanks AM, Spanswick D** 2004 Orexigen-sensitive NPY/AgRP pacemaker neurons in the hypothalamic arcuate nucleus. Nat Neurosci 7:493–494
21. **Nakamura T, Itadani H, Hidaka Y, Ohta M, Tanaka K** 2000 Molecular cloning and characterization of a new human histamine receptor, HH4R. Biochem Biophys Res Commun 279:615–620
22. **Liu C, Wilson SJ, Kuei C, Lovenberg TW** 2001 Comparison of human, mouse, rat, and guinea pig histamine H4 receptors reveals substantial pharmacological species variation. J Pharmacol Exp Ther 299:121–130
23. **Morton GJ, Cummings DE, Baskin DG, Barsh GS, Schwartz MW** 2006 Central nervous system control of food intake and body weight. Nature 443:289–295
24. **Enriori PJ, Evans AE, Sinnayah P, Cowley MA** 2006 Leptin resistance and obesity. Obesity (Silver Spring) 14(Suppl 5):254S–258S
25. **Gottsch ML, Clifton DK, Steiner RA** 2004 Galanin-like peptide as a link in the integration of metabolism and reproduction. Trends Endocrinol Metab 15: 215–221
26. **Revel FG, Ansel L, Klosen P, Saboureau M, Pévet P, Mikkelsen JD, Simonneaux V** 2007 Kisspeptin: a key link to seasonal breeding. Rev Endocr Metab Disord 8:57–65
27. **Jamali AK, Tramu G** 1997 Daily cycle of fos expression within hypothalamic POMC neurons of the male rat. Brain Res 771:45–54
28. **Jamali KA, Tramu G** 1999 Control of rat hypothalamic pro-opiomelanocortin neurons by a circadian clock that is entrained by the daily light-off signal. Neuroscience 93:1051–1061
29. **Sallmen T, Lozada AF, Anichtchik OV, Beckman AL, Panula P** 2003 Increased brain histamine H3 receptor expression during hibernation in golden-mantled ground squirrels. BMC Neurosci 4:24

30. **Panula P, Pirvola U, Auvinen S, Airaksinen MS** 1989 Histamine-immunoreactive nerve fibers in the rat brain. Neuroscience 28:585–610
31. **Inagaki N, Yamatodani A, Ando-Yamamoto M, Tohyama M, Watanabe T, Wada H** 1988 Organization of histaminergic fibers in the rat brain. J Comp Neurol 273:283–300
32. **Pillot C, Pillot C, Heron A, Cochois V, Tardivel-Lacombe J, Ligneau X, Schwartz JC, Arrang JM** 2002 A detailed mapping of the histamine H(3) receptor and its gene transcripts in rat brain. Neuroscience 114:173–193
33. **Ookuma K, Ookuma K, Sakata T, Fukagawa K, Yoshimatsu H, Kurokawa M, Machidori H, Fujimoto K** 1993 Neuronal histamine in the hypothalamus suppresses food intake in rats. Brain Res 628:235–242
34. **Sakata T, Ookuma K, Fujimoto K, Fukagawa K, Yoshimatsu H**1991 Histaminergic control of energy balance in rats. Brain Res Bull 27:371–375
35. **Doi T, Sakata T, Yoshimatsu H, Machidori H, Kurokawa M, Jayasekara LA, Niki N** 1994 Hypothalamic neuronal histamine regulates feeding circadian rhythm in rats. Brain Res 641:311–318
36. **Malmlöf K, Zaragoza F, Golozoubova V, Refsgaard HH, Cremers T, Raun K, Wulff BS, Johansen PB, Westerink B, Rimvall K** 2005 Influence of a selective histamine H3 receptor antagonist on hypothalamic neural activity, food intake and body weight. Int J Obes (Lond) 29:1402–1412
37. **Yoshimoto R, Miyamoto Y, Shimamura K, Ishihara A, Takahashi K, Kotani H, Chen AS, Chen HY, Macneil DJ, Kanatani A, Tokita S** 2006 Therapeutic potential of histamine H3 receptor agonist for the treatment of obesity and diabetes mellitus. Proc Natl Acad Sci USA 103:13866–13871
38. **Leurs R, Bakker RA, Timmerman H, de Esch IJ** 2005 The histamine H3 receptor: from gene cloning to H3 receptor drugs. Nat Rev Drug Discov 4:107–120
39. **Nilaweera KN, Archer ZA, Campbell G, Mayer CD, Balik A, Ross AW, Mercer JG, Ebling FJ, Morgan PJ, Barrett P** 2009 Photoperiod regulates genes encoding melanocortin 3 and serotonin receptors and secretogranins in the dorsomedial posterior arcuate of the Siberian hamster. J Neuroendocrinol 21:123–131